Experimental Verification on Gain Scheduled H_∞ Robust Control of a Magnetic Bearing*

Toru NAMERIKAWA**, Masayuki FUJITA***
and Fumio MATSUMURA**

This paper deals with the problem of gyroscopic effect and unbalance vibration of the Magnetic Bearing system. Using a gain scheduled H_∞ control with a free parameter Φ, we design a control system which attenuates the unbalance vibration, and guarantees the stability against the gyroscopic effect in specified rotational speed. Further we implement the controller and evaluate the effectiveness of the proposed approach by experiments. First, our experimental setup is explained, a mathematical model of the magnetic bearing is derived. Then, we introduce the gain scheduled H_∞ control with free parameters to a magnetic bearing control, in order to reject the disturbances caused by unbalance of the rotor, and guarantee the stability against gyroscopic effect, even if rotational speed of the rotor changes. At last, several experimental results show the effectiveness of this proposed method.

Key Words: Robust Control, Digital Control, Magnetic Bearing, Vibration of Rotating Body, H_∞ Control

1. Introduction

Magnetic bearings are bearings to suspend rotors by magnetic forces without any contact. Around a rotor, several pairs of electromagnets are arranged radially and the rotor can be suspended stably by the active control of magnetic forces. Magnetic bearings have excellent advantages over conventional mechanical bearings. Recent advances in the magnetic bearing technology are covered in the two proceedings of the international symposium on magnetic bearings[1],[2] and a special issue on magnetic bearing control of the IEEE transactions[3].

Both unbalance vibration and gyroscopic effect are serious problems of rigid rotating machines[4]. Unbalance in the rotor mass causes vibration in rotating machines. Balancing of the rotor is very difficult, often there is a residual unbalance. A gyroscopic effect is caused by a coupling of rotor dynamics. This effect can lead to resonances, and often makes the systems unstable.

It is well known that there are two major methods to solve the above unbalance problem of magnetic bearings. The first one is to compensate for the unbalance forces by generating electro-magnetic forces that cancel these forces. The other one is to make the rotor rotate around its axis of inertia (automatic balancing), this approach produces no unbalance forces. There are several effective methods in the literature to achieve automatic balancing in the magnetic bearings[5]-[7]. If the magnetic bearings are applied to precision machines, however, the rotor would be expected to rotate around its geometrical axis, our approach taken here is the first one.

In this paper, we discuss the idea to solve both the problems of the gyroscopic effect and the unbalance vibration by using gain scheduled H_∞ robust control scheme.

We especially focus on the elimination of the variable unbalance vibration caused by a rotational speed. The unbalance vibrations of rigid rotors can be

* Received 13th March, 1997

** Department of Electrical and Computer Engineering, Kanazawa University, 2-40-20 Kodatsuno, Kanazawa 920, Japan

*** School of Information Science, Japan Advanced Institute of Science and Technology, Tatsunokuchi, Ishikawa 923-12, Japan

modeled as frequency-varying sinusoidal disturbances. Hence, our idea is to schedule the peak gain of the controller according to the rotational frequency of the rotor to make the system possess high stiffness at the operation speed.

This gain scheduling algorithm is very simple and utilizes the free parameter of the H_∞ controller[8]. The other gain-scheduling approaches for H_∞ control are reported in references[9]-[11] and its application result has been reported in Ref.(12). The advantage of this approach is a good performance at the operating point comparing with the other approaches[9]-[11], but this approach can not be applied to wide parameter space which is a disadvantage.

For the problem of gyroscopic effect, we utilize the small gain theorem to make the stability margin clear.

This paper is a continuation of the previous research[13]. We have especially improved the interpolation accuracy of the controller and described the detail of interpolation, implementation and experimental results of the proposed method.

Outline of this paper is as follows. First, we introduce the magnetic bearing system, and derive the mathematical model of the system[14],[15]. Next, we adopt the H_∞ problem with boundary constraints to the normalized left coprime factor robust stabilization H_∞ problem[8], the conditions for existence of controller are derived with LSDP[16]. Third, we design the controllers that achieve asymptotic disturbance rejection and robust stability. At last, we present experimental results with the obtained H_∞ controllers, and indicate the effectiveness of this proposed approach.

2. Modeling

2.1 Magnetic bearing system

The magnetic bearing system employed in this research is a 4-axis controlled horizontal shaft magnetic bearing with symmetrical structure. The axial motion is not controlled actively. The diagram of the experimental machine is shown in Fig. 1. The diameter of the rotor is 96 mm, its span is 660 mm, and its mass is 13.9 kg. A three-phase induction motor (1kW, four poles) is located at the center of the rotor. Around the rotor, four pairs of electromagnets are arranged radially. All physical parameters are listed in Table 1. Four pairs of eddy-current type gap sensors are located on outside of the electromagnets. A tachometer is arranged on the side of the rotor to measure the rotational speed.

2.2 Mathematical model of the magnetic bearing

In order to derive the state equation of a magnetic bearing, the following assumptions are made.

Table 1 Parameters of experimental machine

Parameter	Symbol	Value	Unit
Mass of the Rotor	m	1.39×10^{1}	kg
Moment of Inertia about X	J_x	1.348×10^{-2}	kg · m^2
Moment of Inertia about Y	J_y	2.326×10^{-1}	kg · m^2
Distance between Center of Mass and Left Electromagnet	l_l	1.30×10^{-1}	m
Distance between Center of Mass and Right Electromagnet	l_r	1.30×10^{-1}	m
Distance between Center of Mass and Motor	l_m	0	m
Steady Attractive Force	$F_{l1,r1}$	9.09×10	N
	$F_{l2\sim l4}$	2.20×10	N
	$F_{r2\sim r4}$	2.20×10	N
Steady Current	$I_{l1,r1}$	6.3×10^{-1}	A
	$I_{l2\sim l4}$	3.1×10^{-1}	A
	$I_{r2\sim r4}$	3.1×10^{-1}	A
Steady Gap	W	5.5×10^{-4}	m
Resistance	R	1.07×10	Ω
Inductance	L	2.85×10^{-1}	H

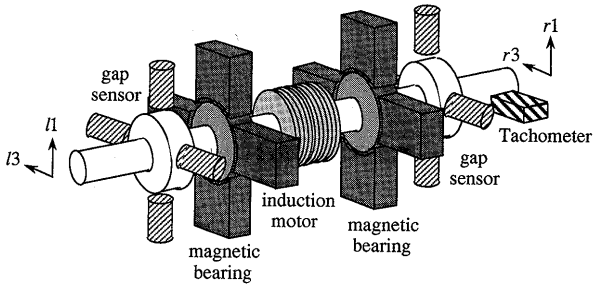

Fig. 1 Diagram of experimental machine

1. The rotor is rigid and has no unbalance.
2. All electromagnets are identical.
3. Attractive force of an electromagnet is in proportion to (electric current/gap length)^2.
4. The resistance and the inductance of the electromagnet coil are constant and independent of the gap length.
5. Small deviations from the equilibrium point are treated.

Based on the above assumptions, a mathematical model of a magnetic bearing has been derived in Ref. (15), and the result obtained is as follows.

$$\begin{bmatrix}\dot{x}_v\\ \dot{x}_h\end{bmatrix}=\begin{bmatrix}A_v & pA_{vh}\\ -pA_{vh} & A_h\end{bmatrix}\begin{bmatrix}x_v\\ x_h\end{bmatrix}+\begin{bmatrix}B_v & 0\\ 0 & B_h\end{bmatrix}\begin{bmatrix}u_v\\ u_h\end{bmatrix}+p^2\begin{bmatrix}E_v\\ E_h\end{bmatrix}w \quad (1)$$

$$\begin{bmatrix}y_v\\ y_h\end{bmatrix}=\begin{bmatrix}C_v & 0\\ 0 & C_h\end{bmatrix}\begin{bmatrix}x_v\\ x_h\end{bmatrix} \quad (2)$$

where the subscripts 'v' and 'h' in the vectors and the matrices stand for the vertical motion and the horizontal motion respectively of the magnetic bearing. In addition, the subscript 'vh' stands for the coupling term between the vertical motion and the horizontal motion, and p denotes the rotational speed of the rotor. In Eq.(1), terms $\{pA_{vh}, -pA_{vh}\}$ are gyroscopic

effects and $\{p^2E_v,\ p^2E_h\}$ are unbalance terms, which are functions of p.

Each vector in Eqs.(1) and (2) is defined as

$$x_v=[g_{l1}\quad g_{r1}\quad \dot{g}_{l1}\quad \dot{g}_{r1}\quad i_{l1}\quad i_{r1}]^T,$$
$$x_h=[g_{l3}\quad g_{r3}\quad \dot{g}_{l3}\quad \dot{g}_{r3}\quad i_{l3}\quad i_{r3}]^T,$$
$$u_v=[e_{l1}\quad e_{r1}]^T,\ u_h=[e_{l3}\quad e_{r3}]^T,$$
$$w=\begin{bmatrix}\varepsilon\sin(pt+\kappa)\\ \tau\cos(pt+\lambda)\\ \varepsilon\cos(pt+\kappa)\\ \tau\sin(pt+\lambda)\end{bmatrix} \tag{3}$$

where

g_j : deviations from the steady gap lengths between the electromagnets and the rotor

i_j : deviations from the steady currents of the electromagnets

e_j : deviations from the steady voltages of the electromagnets

$\varepsilon, \tau, \kappa, \lambda$: unbalance parameters[15],[17]

$(j=l1,\ r1,\ l3,\ r3.)$

The subscripts 'l' and 'r' denote the left-hand side and the right-hand side of the rotor respectively, and the subscripts '1' and '3' denote one of the vertical directions and one the horizontal directions of the rotor respectively. Each elemental matrix in Eqs.(1) and (2) is defined in Appendix A.

3. H_∞ Gain Scheduling

In order to attenuate the unbalance vibration and guarantee the stability against gyroscopic effect, we utilize the H_∞ controller and its free parameter.

The unbalance vibrations can be modeled as frequency-varying sinusoidal force disturbances. Hence, the idea here is to schedule the controller's peak gain according to the rotational frequency to possess the system high stiffness at the operation speed. As is well known, if a controller has imaginary poles at a certain frequency, it possess high gain/stiffness at corresponding frequency. Hence we measure the rotational speed p and change the poles of a free parameter of the H_∞ control, we can make the H_∞ controller to have high gain[8].

For the problem of gyroscopic effect, we utilize the small gain theorem to make the stability margin clear.

We therefore show the condition for existing of free parameter, by adopting the control problem with boundary constraints[8] to the normalized left coprime factorization robust stabilization problem, and we design a robust controller which satisfies the derived specifications by LSDP[16].

3.1 Loop shaping based H_∞ synthesis

Let (N, M) represent a normalized left coprime factorization of a plant G. Let these coprime factors be assumed to have uncertainties Δ_N, Δ_M and let G_Δ represent the plant with these uncertainties.

$$G_\Delta=M_\Delta^{-1}N_\Delta$$
$$=(M+\Delta_M)^{-1}(N+\Delta_N) \tag{4}$$

where N_Δ and M_Δ represent a left coprime factorization of G_Δ, and

$$\Delta=\{[\Delta_N,\ \Delta_M]\in RH_\infty\ ;\ \|[\Delta_N,\ \Delta_M]\|_\infty<\varepsilon\}. \tag{5}$$

G_Δ can be written in the form of an upper linear fractional transformation (ULFT) as follows.

$$G_\Delta=F_U(P,\ \Delta)$$
$$=P_{22}+P_{21}\Delta(I-P_{11}\Delta)^{-1}P_{12}, \tag{6}$$

where

$$P=\left[\begin{array}{c|c}P_{11} & P_{12}\\ \hline P_{21} & P_{22}\end{array}\right]=\left[\begin{array}{c|c}0 & I\\ \hline M^{-1} & G\end{array}\right]. \tag{7}$$

The robust stabilization problem for the *perturbed* plant G_Δ can be treated as the next H_∞ control problem:

$$\left\|\begin{bmatrix}K\\ I\end{bmatrix}(I-GK)^{-1}M^{-1}\right\|_\infty\le\varepsilon^{-1}:=\gamma \tag{8}$$

It is well known that the solution of this problem and the largest number of ε $(=\varepsilon_{\max}:=\gamma_{\min}^{-1})$ can be obtained by solving two Riccati equations without iteration. All controllers K satisfying Eq.(8) are given by

$$K=F_L(K_a,\ \Phi):=K_{11}+K_{12}\Phi(I-K_{22}\Phi)^{-1}K_{21}, \tag{9}$$

where

$$K_a=\left[\begin{array}{c|c}K_{11} & K_{12}\\ \hline K_{21} & K_{22}\end{array}\right],\ \|\Phi\|_\infty\le1. \tag{10}$$

For the calculation of K_a and $\varepsilon_{\max}$, see Ref.(16).

3.2 Elimination of unbalance vibration

Unbalance vibration can be modeled as sinusoidal disturbance[18], the robust controller should be designed to reject this disturbance.

As is well known, if the controller would have the imaginary poles at the frequencies corresponding to the rotational speed, it has a peak gain at this point. Hence, $K(s)$ is required to satisfy

$$K(\pm j\omega_0)=\infty\Leftrightarrow\{I-G(\pm j\omega_0)K(\pm j\omega_0)\}^{-1}=0, \tag{11}$$

where ω_0 is frequency of rotation.

3.3 H_∞ controller with free parameter

Adopting the H_∞ problem with boundary constraints[8] (in Appendix B) to this problem, we derive the condition that a controller satisfying both Eqs.(8) and (11) exists.

The boundary constraint $\{L, \Pi, \Psi\}$ corresponding to Eq.(11) is given by

$$L=[0\quad I],\ \Pi=M(\pm j\omega_0),\ \Psi=0. \tag{12}$$

The basic constraint $\{L_B,\ \Psi_B\}$ in Eq.(34) (Appendix B) is described by

$$L_B=P_{12}^{\perp}(\pm j\omega_0)=[-G(\pm j\omega_0)\quad I], \tag{13}$$

$$\Psi_B = P_{12}^{\perp}(\pm j\omega_0)P_{11}(\pm j\omega_0) = M^{-1}(\pm j\omega_0). \quad (14)$$

It is obvious that $\{L, \Pi, \Psi\}$ is satisfying condition (b) in Theorem A, and the extended boundary constraint $\{\hat{L}, \hat{\Psi}\}$ in Eq.(35) (Appendix B) is given by

$$\hat{L} = \begin{bmatrix} -G(\pm j\omega_0) & I \\ 0 & I \end{bmatrix}, \quad \hat{\Psi} = \begin{bmatrix} I \\ 0 \end{bmatrix}. \quad (15)$$

After some straightforward calculation, we have

$$\gamma\bar{\sigma}(N(\pm j\omega_0)) > 1, \quad (16)$$

where

$$\bar{\sigma}(N(\pm j\omega_0)) = \left(\frac{\bar{\sigma}^2(G(\pm j\omega_0))}{1+\bar{\sigma}^2(G(\pm j\omega_0))}\right)^{1/2},$$

$\bar{\sigma}(\bullet)$: the maximum singular value,

from the condition (c) of Theorem A.

If we choose free parameter $\Phi(s)$ such that

$$\Phi(\pm j\omega_0) = K_{22}^{-1}(\pm j\omega_0) \quad (17)$$

under the conditions Eqs.(10) and (16), it can be seen that we obtain the controller with the imaginary poles at $\pm j\omega_0$ from Eq.(9). Based on it, we design the control system using the loop shaping design procedure[16]. This is briefly outlined in Appendix C. Thus, we can design the robust controllers achieving sinusoidal disturbance rejection. Utilizing the free parameter of H_∞ controller, the controller's gain is scheduled by the rotational speed.

4. Controller Design

In this section, we design the feedback controllers by LSDP. At first, we assume rotational speed $p=0$ in the nominal plant G. In this case, there is no coupling between the vertical motion and horizontal motion in Eq.(1). Finally, the coupling between the vertical and the horizontal motion has been included in the design.

The plant model can be separated into the vertical plant $G_v(s) := C_v(sI-A_v)^{-1}B_v$ and the horizontal plant $G_h(s) := C_h(sI-A_h)^{-1}B_h$, respectively.

$$G = \begin{bmatrix} G_v & 0 \\ 0 & G_h \end{bmatrix} \quad (18)$$

Thus, two controllers are designed for each plant respectively. The final controller K for the entire plant G is constructed with the combination of these two controllers.

$$K = \begin{bmatrix} K_v & 0 \\ 0 & K_h \end{bmatrix} \quad (19)$$

where K_v and K_h denote the controller for the vertical plant and the horizontal plant respectively.

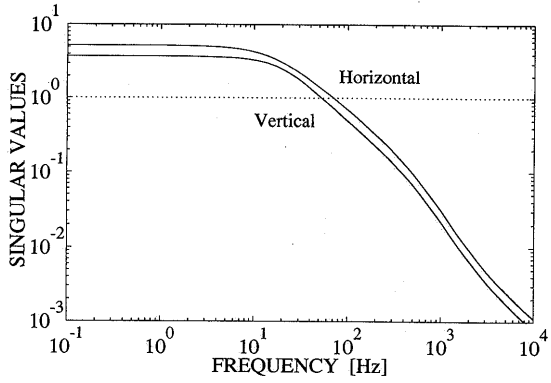

(a) Magnitude of $\gamma\sigma(Ns)$

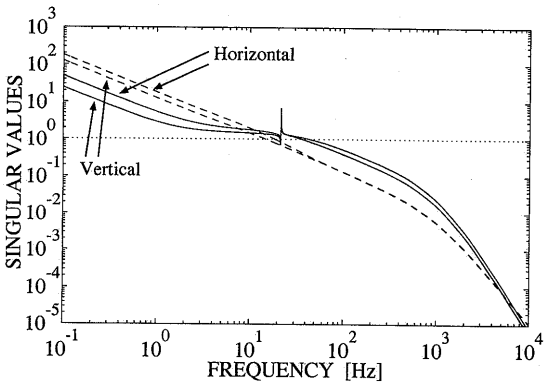

(b) Open loop transfer functions GK[——] and the shaped plant Gs[— —]

Fig. 2 Characteristics of the H_∞ controller $K(s)$

4.1 LSDP design parameter

After some experimental trial and error, final results of the design iterations are as follows.

(v) Design for vertical motion

$$W_{1v}(s) = \frac{1\,300(1+s/(2\pi\cdot 5))(1+s/(2\pi\cdot 35))(1+s/(2\pi\cdot 50))}{(1+s/(2\pi\cdot 0.01))(1+s/(2\pi\cdot 700))(1+s/(2\pi\cdot 1\,200))}\begin{bmatrix} 1 & 0 \\ 0 & 1 \end{bmatrix} \quad (20)$$

$$W_{2v}(s) = 10\,000\begin{bmatrix} 1 & 0 \\ 0 & 1 \end{bmatrix} \quad (21)$$

$$\varepsilon_{v\_max} = 0.199\,44,\ \varepsilon_v^{-1} = \gamma_v = 5.25 \quad (22)$$

(h) Design for horizontal motion

$$W_{1h}(s) = \frac{1\,100(1+s/(2\pi\cdot 5))(1+s/(2\pi\cdot 25))(1+s/(2\pi\cdot 40))}{(1+s/(2\pi\cdot 0.01))(1+s/(2\pi\cdot 700))(1+s/(2\pi\cdot 1\,200))}\begin{bmatrix} 1 & 0 \\ 0 & 1 \end{bmatrix} \quad (23)$$

$$W_{2h}(s) = 100\,00\begin{bmatrix} 1 & 0 \\ 0 & 1 \end{bmatrix} \quad (24)$$

$$\varepsilon_{h\_max} = 0.274\,32,\ \varepsilon_h^{-1} = \gamma_h = 3.75. \quad (25)$$

The problem of LSDP is that the order of the controller becomes high. Hence we employed a model

Table 2 Parameters a_d, b_d of free parameters

Rotational speed (rpm)	a_v	b_v	a_h	b_h
1000 ~ 1600	2800	8	2800	8
1600 ~ 2200		16		16
2200 ~ 2600	2500	25	2500	27
2600 ~ 2900		37		36
2900 ~ 3100				40

reduction technique[16]. The order of the each shaped plant is reduced from 12 states to 8, then, the final controller has 36 states.

Characteristics of the obtained H_∞ controller K are shown in Fig. 2. From Fig. 2(a), it can be seen that the Φ in Eq.(17) exists below $\omega_0=324.63$ [rad/s] ($p=3100$ [rpm]) by the condition in Eq.(16). Hence we design a controller within the above limit. In order to satisfy the conditions Eqs. (10) and (16), the free parameters are selected as

$$\Phi_d(s)=C_{\Phi d}(sI-A_{\Phi d})^{-1}B_{\Phi d}, \tag{26}$$

where

$$A_{\Phi d}=\begin{bmatrix}-a_d & 0\\ 0 & -b_d\end{bmatrix},\ B_{\Phi d}=\begin{bmatrix}I\\ I\end{bmatrix},\ C_{\Phi d}=[C_{\Phi 1d}\quad C_{\Phi 2d}],$$

$$C_{\Phi 1d}=\frac{(a_d^2+\omega_0^2)}{\omega_0(a_d-b_d)}\{\omega_0\Re(K_{22d}^{-1}(j\omega_0))+b_d\Im(K_{22d}^{-1}(j\omega_0))\},$$

$$C_{\Phi 2d}=\frac{(b_d^2+\omega_0^2)}{\omega_0(b_d-a_d)}\{\omega_0\Re(K_{22d}^{-1}(j\omega_0))+a_d\Im(K_{22d}^{-1}(j\omega_0))\}.$$

$(d=v,\ r)$

Furthermore, in order to satisfy the condition in Eq. (10), the parameters a_d, b_d of $A_{\Phi d}$ and $C_{\Phi d}$ are adjusted as in Table 2.

We show the gain-scheduled H_∞ controller at $\omega_0=136.14$ [rad/s] ($p=1300$ [rpm]) as a design example. The singular values of the shaped plants and the open loop transfer functions are shown in Fig. 2(b). We can see that the controller has the peak gain at $\omega_0=136.14$ [rad/s].

4.2 Validity of the performance and stability

Figure 3 shows the singular values of the closed-loop characteristics.

The sensitivity functions $\sigma((I-GK)^{-1})$ are plotted in Fig. 3(a), and we can see that the sensitivity approaches zero at the frequency $\omega_0(=136.14)$ from this figure. This result shows the good property to eliminate unbalance vibration.

In this design process, we ignored the interference terms, which express the gyroscopic effect, as $p=0$. We therefore verify the robust stability of the closed-loop system against changes in the rotational speed. Let the perturbed plant ($p\neq 0$) be denoted by G_p and the additive perturbation Δ_p of G is as follows.

$$\Delta_p=G_p-G \tag{27}$$

Then the robust stability is guaranteed within the following inequality Eq.(28).

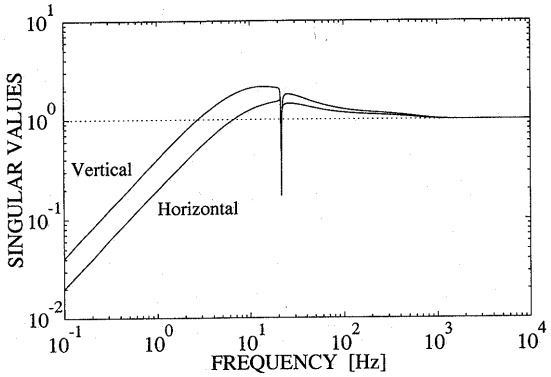

(a) $\sigma((I-GK)^{-1})$

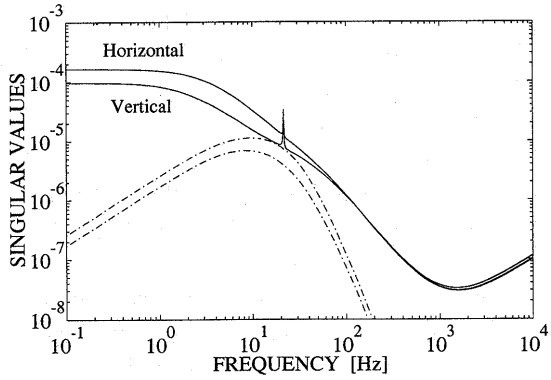

(b) $1/\sigma(K(I-GK)^{-1})$[——] and $\sigma(\Delta_p)$[— • —]

Fig. 3 Validity of the closed-loop system

$$\bar{\sigma}(\Delta_p)<\frac{1}{\bar{\sigma}(K(I-GK)^{-1})} \tag{28}$$

In Fig. 3(b), the singular values $1/\sigma(K(I-GK)^{-1})$ and $\sigma(\Delta_p)$ at $\omega_0=1675.5$ [rad/s] ($p=16000$ [rpm]) are plotted. From this analyzed results, the closed-loop system is confirmed to be stable below $\omega_0\leq 1675.5$ [rad/s].

5. Experimental Results

In this section, we validate the obtained controller by experiments.

5.1 Digital control system

The experimental machine is controlled by a digital control system that consists of a 32-bit floating point Digital Signal Processor (DSP) DSP 32C (AT & T), 12-bit A/D converters and 12-bit D/A converters. Using these components, the final discrete-time controllers including a free parameter are computed on the DSP.

5.2 Implementation of the gain scheduled H_∞ controller

The obtained controller has 36 orders and is a continuous system. We discretized them via the well known Tustin transform.

The discrete-time controller $K_d(z)$ is shown as follows.

$$K_d(z)=\left[\begin{array}{c|c} A_{kd} & AP_{kd}(p) \mid BP_{kd}(p) \\ \hline C_{kd} & CP_{kd}(p) \mid DP_{kd}(p) \end{array}\right], \quad (29)$$

where $A_{kd}\in R^{18\times 6}$, $AP_{kd}(p)\in R^{18\times 12}$, $BP_{kd}(p)\in R^{18\times 2}$, $C_{kd}\in R^{2\times 6}$, $CP_{kd}(p)\in^{2\times 12}$, $DP_{kd}(p)\in R^{2\times 2}$.

Here A_{kd} and C_{kd} are constant matrices, on the other hand, AP_{kd}, BP_{kd}, CP_{kd}, and DP_{kd} are functions of the rotational speed p.

The above four matrices with p are so complicated, that we implement the each element of them by using polynomial approximation in real-time calculation.

In order to shorten the sampling period, we employed the 2nd order polynomial approximation by the least-square method, which is as follows.

$$AP_{kd}(p)=p^2A_{d2}+pA_{d1}+A_{d0}, \quad (30)$$

$$BP_{kd}(p)=p^2B_{d2}+pB_{d1}+B_{d0}, \quad (31)$$

$$CP_{kd}(p)=p^2C_{d2}+pC_{d1}+C_{d0}, \quad (32)$$

$$DP_{kd}(p)=p^2D_{d2}+pD_{d1}+D_{d0}, \quad (33)$$

where $\{A, B, C, D\}_{d2}$, $\{A, B, C, D\}_{d1}$ and $\{A, B, C, D\}_{d0}$ are constant matrices of 2nd-order, 1st-order, and constant, respectively.

We show an example of this approximation in Fig. 4. This figure shows the $AP_{kd11}(p)$, which is a 1−1 element of $AP_{kd}(p)$. The horizontal axis is the rotational speed from 1 000 to 1 600 rpm, the vertical axis shows the magnitude, and the symbols '×' mean the real values calculated with every 25 rpm, and the solid line shows the 2nd order approximated interpolated function of '×'s.

These approximations are done for the all (18×12 +18×2+2×12+2×2) elements of $\{AP_{kd}, BP_{kd}, CP_{kd}, DP_{kd}\}$.

Very often the gain-scheduling of the controller is realized via convex parametrization of the two controller at the end points. In Ref. (13), this method was also employed. This is very simple but the interpolation is not so precise. In this paper, the polynomial approximation was employed and it improved the precision of interpolation of the gain scheduled controller.

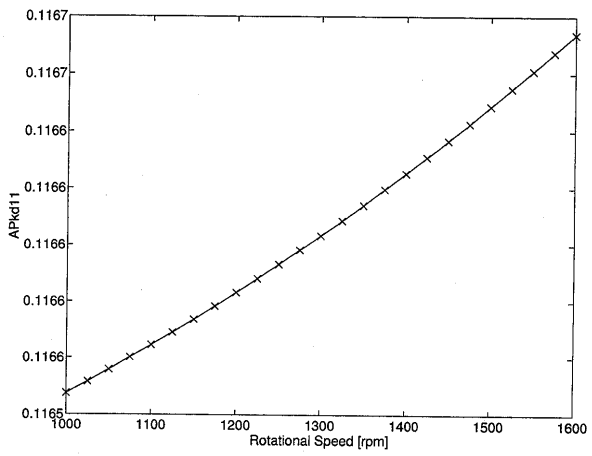

Fig. 4 Polynomial approximation of $AP_{kd_{11}}(p)$

5.3 Experimental condition

We have carried out experiments using the experimental machine shown in Fig. 1. In order to evaluate the practical effect of this proposed approach, the experimental tests were run within the limits of the rotational speed from 1 000 to 1 600 rpm (see Table 2).

The designed continuous-time controllers, K_{1300} and Gain Scheduled H_∞ Controller are discretized via the well known Tustin transform at the sampling rates of 252 μs and 415 μs, respectively.

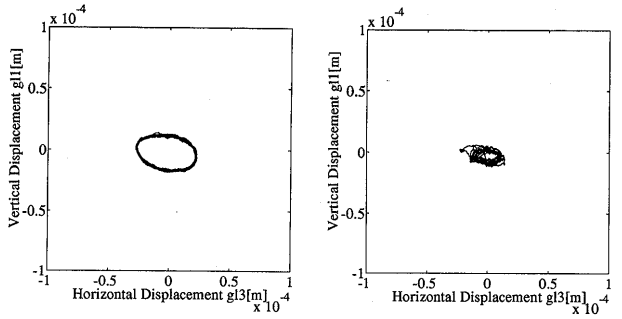

(a 1) Fixed H_∞ controller K_{1300} : rotational speed 1 100 [rpm]

(a 2) Gain scheduled H_∞ controller : rotational speed 1 100 [rpm]

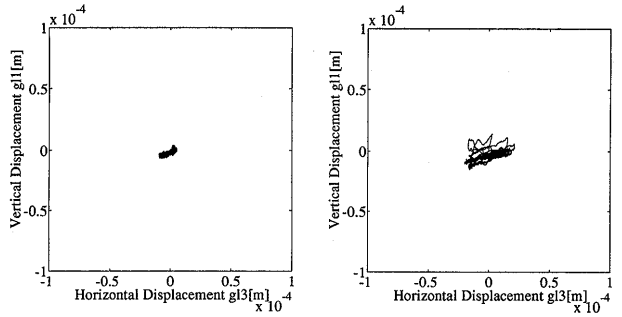

(b 1) Fixed H_∞ controller K_{1300} : rotational speed 1 300 [rpm]

(b 2) Gain scheduled H_∞ controller : rotational speed 1 300 [rpm]

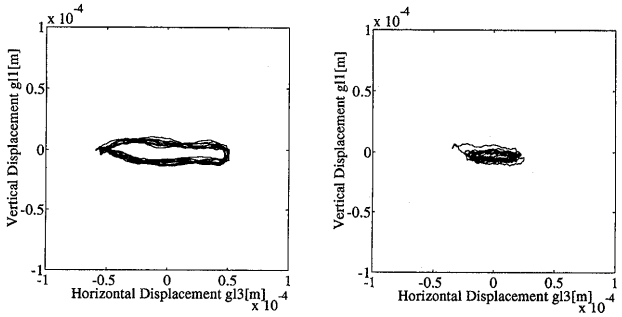

(c 1) Fixed H_∞ controller K_{1300} : rotational speed 1 500 [rpm]

(c 2) Gain scheduled H_∞ controller : rotational speed 1 500 [rpm]

Fig. 5 Orbits of the physical center of the rotor

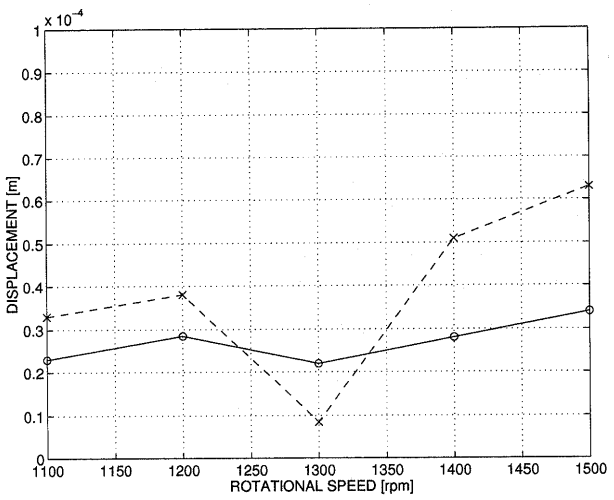

Fig. 6 Unbalance responses against the rotational frequency

The controller K_{1300} is linear time-invariant dynamical controller, hence the computing burden for real-time calculation of control input is only matrix multiplication and addition. On the other hand, for the implementation of the gain scheduled H_∞ controller $K(\Phi)$, however, we have to renew $K(\Phi)$ from Eqs. (30), (31), (32) and (33) by every sampling period. After it has been obtained, the control input u is calculated. It takes longer time to implement $K(\Phi)$.

All through the experiments, a small weight (20[g]) is attached at the side of the rotor of the opposite side of the tachometer in Fig. 1. This weight is introduced to increase the residual unbalance.

We have measured the orbits of the physical center of the rotor on the perpendicular plane for a period of 0.5 s under several rotational conditions. Figures 5(a 1), 5(b 1) and 5(c 1) show the results with K_{1300}, and Fig. 5(a 2), 5(b 2) and 5(c 2) show the results with the gain scheduled controller $K(\Phi)$ at 1 100, 1 300 and 1 500 rpm, respectively.

Further the unbalance responses against the rotational frequency are given in Fig. 6. The vertical axis shows the maximum displacement from the physical center in radial plane, where the solid line shows the result with gain scheduled controller, and the dashed line shows the fixed controller.

5.4 Evaluation and consideration

Compared the gain scheduled H_∞ controller $K(\Phi)$ with the fixed H_∞ controller K_{1300}, the results with $K(\Phi)$ indicate better performance than the one with K_{1300} in the elimination of the unbalance vibration except at 1 300 rpm.

These results in Fig. 5 and Fig. 6 show the effectiveness of the gain schedule method for changing rotational speed.

However, it is well known that direct switching and interpolation between the controllers does not capture the dynamic effects and may lead to instability, even if the controllers can stabilize the closed-loop system for each frozen value in the parameter space. This is especially true if the scheduled parameter changes rapidly. By the numerical simulation, we have confirmed that the closed-loop system is stable when the rotational speed changes below the rate of 10 rpm/s. We found a example that if the rotational speed changes more than 10 rpm/s the system becomes unstable.

While the rotor speed should be able to vary, for many applications it does not need to vary quickly. For this rotor, limited power and the safety of the induction motor dictate that the rotational speed can not be changed rapidly.

From a theoretical point of view, gain scheduled H_∞ controller should completely attenuate the unbalance vibration even if the rotational speed varies. However, this level of performance has not been achieved experimentally. This performance deterioration may be due to the measurement precision of the rotating speed. Gain scheduled H_∞ controller strongly relies on the accuracy of the rotational speed. Since the notch in the sensitivity function is very narrow, error in the measurement of rotational speed may significantly deteriorate performance.

Further investigation and experiments examining the effects of rotational speed and the scheduled parameter's changing rate, will be made in the future.

6. Conclusion

In this paper, we proposed a gain scheduled H_∞ robust control scheme with free parameters for the elimination of unbalance vibration in a magnetic bearing supported rotor. We treated the changing unbalance vibration caused by varying rotational speed as a known frequency-varying disturbance, and adjusted the controller gain according to the rotational speed of the rotor using the free parameter Φ of the H_∞ controller. The obtained controller $K(\Phi)$ has high gain at the operating frequency.

First, the dynamics of the AMB system was considered and a nominal mathematical model for the system was derived. Next, the conditions for the existence of controllers were derived, and, we designed the gain scheduled H_∞ robust controllers using LSDP. It rejected the sinusoidal disturbance of the varying rotor speed.

Finally experimental results showed the effectiveness of this proposed method.

Appendix A

Matrices in Eqs.(1) and (2) are defined as

$$A_v := \begin{bmatrix} 0 & I & 0 \\ A_1+A_2A_{4v} & 0 & A_2A_{5v} \\ 0 & 0 & -(R/L)I \end{bmatrix},$$

$$A_h := \begin{bmatrix} 0 & I & 0 \\ A_1+A_2A_{4h} & 0 & A_2A_{5h} \\ 0 & 0 & -(R/L)I \end{bmatrix},$$

$$A_{vh} := \begin{bmatrix} 0 & 0 & 0 \\ 0 & A_3 & 0 \\ 0 & 0 & 0 \end{bmatrix},\ B_v=B_h := \begin{bmatrix} 0 \\ 0 \\ (1/L)I \end{bmatrix},$$

$$C_v=C_h := [I \quad 0 \quad 0],\ E_v := \begin{bmatrix} 0 \\ E_{1v} \\ 0 \end{bmatrix},\ E_h := \begin{bmatrix} 0 \\ E_{1h} \\ 0 \end{bmatrix},$$

$$A_1 := \frac{\alpha}{l_l+l_r}\begin{bmatrix} (l_r-l_m)\left(\frac{1}{m}-\frac{l_ll_m}{J_y}\right) & (l_l-l_m)\left(\frac{1}{m}-\frac{l_ll_m}{J_y}\right) \\ (l_r-l_m)\left(\frac{1}{m}+\frac{l_rl_m}{J_y}\right) & (l_l-l_m)\left(\frac{1}{m}+\frac{l_rl_m}{J_y}\right) \end{bmatrix},$$

$$A_2 := \begin{bmatrix} -\frac{1}{m}-\frac{l_l^2}{J_y} & -\frac{1}{m}+\frac{l_ll_r}{J_y} \\ -\frac{1}{m}+\frac{l_ll_r}{J_y} & -\frac{1}{m}-\frac{l_r^2}{J_y} \end{bmatrix},$$

$$A_3 := \frac{J_x}{J_y(l_l+l_r)}\begin{bmatrix} -l_l & l_l \\ l_r & -l_r \end{bmatrix},$$

$$A_{4v} := -\frac{2}{W}\mathrm{diag}[F_{l1}+F_{l2},\ F_{r1}+F_{r2}],$$

$$A_{4h} := -\frac{2}{W}\mathrm{diag}[F_{l3}+F_{l4},\ F_{r3}+F_{r4}],$$

$$A_{5v} := 2\mathrm{diag}\left[\frac{F_{l1}}{I_{l1}}+\frac{F_{l2}}{I_{l2}},\ \frac{F_{r1}}{I_{r1}}+\frac{F_{r2}}{I_{r2}}\right],$$

$$A_{5h} := 2\mathrm{diag}\left[\frac{F_{l3}}{I_{l3}}+\frac{F_{l4}}{I_{l4}},\ \frac{F_{r3}}{I_{r3}}+\frac{F_{r4}}{I_{r4}}\right],$$

$$E_{1v} := \begin{bmatrix} -1 & l_l\left(1-\frac{J_x}{J_y}\right) & 0 & 0 \\ -1 & -l_r\left(1-\frac{J_x}{J_y}\right) & 0 & 0 \end{bmatrix},$$

$$E_{1h} := \begin{bmatrix} 0 & 0 & 1 & l_l\left(1-\frac{J_x}{J_y}\right) \\ 0 & 0 & 1 & -l_r\left(1-\frac{J_x}{J_y}\right) \end{bmatrix},$$

For the notations, as well as the parameter values, see Table 1. In the above equations, α denotes the coefficient of the force which occurs when the rotor eccentrically deviates, and hence we set $\alpha=0$. The numerical values of these matrices can be easily obtained with Table 1, and the result is written in Ref. (14).

Appendix B

● Definition A. "H_∞ problem with boundary constraints"

Find the $K(s)$ satisfying

(s 1) $K(s)$ stabilizes $F_U(P, 0)$,

(s 2) $\|P_{zw}\|_\infty \leq \varepsilon^{-1} := \gamma$, where $P_{zw}=F_L(P, K)$,

(s 3) $LP_{zw}(j\omega)\Pi=\Psi$.

● Definition B. "Basic constraints"

$$L_B := P_{12}^{\perp}(j\omega),\ \Psi_B := P_{12}^{\perp}(j\omega)P_{11}(j\omega),$$
$$P_{12}^{\perp}(s)P_{12}(s)=0. \tag{34}$$

● Definition C. "Extended constraints"

$$\hat{L} := \begin{bmatrix} L_B \\ L \end{bmatrix},\ \hat{\Psi} := \begin{bmatrix} \Psi_B\Pi \\ \Psi \end{bmatrix} \tag{35}$$

where $\hat{L}$ and $\hat{\Psi}$ are row full rank.

Theorem A.

H_∞ problem with boundary constraints $\{L, \Pi, \Psi\}$ is solvable, iff the following three conditions hold:

(a) The H_∞ problem is solvable.

(b) $\mathrm{rank}\begin{bmatrix} L_B & \Psi_B\Pi \\ L & \Psi \end{bmatrix}=\mathrm{rank}\begin{bmatrix} L_B \\ L \end{bmatrix}$

(c) $\hat{L}\hat{L}^* > \gamma^2\hat{\Psi}(\Pi^*\Pi)^{-1}\hat{\Psi}^*$.

Appendix C

Loop Shaping Design Procedure (LSDP)

<Step 1>Loop Shaping

Selecting shaping function W_1 and W_2, the singular values of the nominal plant G are shaped to have a desired open loop shape. Let G_S represent this shaped plant

$$G_S=W_2GW_1 \tag{36}$$

W_1 and W_2 should be selected such that G_S has no hidden unstable modes.

<Step 2>Robust Stabilization

The maximum stability margin $\varepsilon_{\max}$ is calculated. If $\varepsilon_{\max} \ll 1$, return to Step 1, then W_1 and W_2 should be selected again. Otherwise, γ is appropriately selected as $\gamma \geq \gamma_{\min}=\varepsilon_{\max}^{-1}$ and K_a is calculated. The free parameter Φ is selected such as Eq. (17). The H_∞ controller: $K_\infty(s)$ is synthesized for G_S from Eq. (9).

<Step 3>Final Controller

The final controller K can be obtained by the combination of W_1, W_2 and K_∞

$$K=W_1K_\infty W_2 \tag{37}$$

References

(1) Schweitzer, G., Ed., Proc. Fourth Int. Symp. Magnetic Bearings, Zurich, Switzerland, Aug., 1994.

(2) Matsumura, F., Ed., Proc. Fifth Int. Symp. Magnetic Bearings, Kanazawa, Japan, Aug., 1996.

(3) Knospe, C. R. and Collins, E. G., Ed., IEEE Trans. on Cont. Sys. Tech. Special Issue on Magnetic Bearing Control, Vol. 4, No. 5, Sep., 1996.

(4) Knospe, C. R., Robustness of Unbalance Response Controllers, Proc. of 3rd International Symposium on Magnetic Bearings, Virginia, July, 1992.

(5) Shafai, B., Beale, S., LaRocc, P. and Cusson, E., Magnetic Bearing Control Systems and Adaptive Forced Balancing, IEEE Control Systems Magazine, vol. 14, No. 2(1994), p. 4-13.

(6) Mohamed, A. M. and Busch-Vishniac, I. J., Imbalance Compensation and Automation Balancing in Magnetic Bearing Systems Using the Q-Par-

ameterization Theory, IEEE Trans. on Control Systems Technology, Vol. 3, No. 2(1995), p. 202-211.
(7) Mizuno, T. and Higuchi, T., Compensation for Unbalance in Magnetic Bearing Systems, Trans. of SICE, (in Japanese), Vol. 20, No. 12(1984), p. 23-29.
(8) Sugie, T. and Hara, S., H_∞-Suboptimal Control Problem with Boundary Constraints, Systems & Control Letters, Vol. 13 (1989), p. 93-99.
(9) Apkarian, P., Gahinet, P. and Becker, G., Self-Scheduled H_∞ Control of Linear Parameter-Varying Systems, Proc. of American Control Conference, (1994), p. 856-860.
(10) Nichols, R. A., Reichert, R. T. and Rugh, W. J., Gain Scheduling for H_∞ Controllers: A Flight Control Example, IEEE Transactions on Control Systems Technology, Vol. 1, No. 2(1993), p. 69-79.
(11) Packard, A., Gain Scheduling via Linear Fractional Transformations, Systems & Control Letters, Vol. 22, No. 2(1994), p. 79-92.
(12) Sivrioglu, S. and Nonami, K., LMI Based Gain Scheduled H_∞ Controller Design for AMB Systems under Gyroscopic and Unbalance Disturbance Effect, Proc. 5th Int. symp. on Magnetic Bearings, Kanazawa, Japan, (1996), p. 191-196.
(13) Matsumura, F., Namerikawa, T., Hagiwara, K. and Fujita, M., Application of Gain Scheduled H_∞ Robust Controllers to a Magnetic Bearing, IEEE Trans. on Cont. Sys. Tech., Vol. 4, No. 5(1996), p. 484-492.
(14) Fujita, M., Hatake, K. and Matsumura, F., Loop Shaping Based Robust Control of a Magnetic Bearing, IEEE Control Systems Magazine, Vol. 13, No. 4(1993), p. 57-65.
(15) Matsumura, F., Kobayashi, H. and Akiyama, Y., Fundamental Equation of Horizontal Shaft Magnetic Bearing and its Control System Design, Trans. IEE of Japan, (in Japanese), Vol. 101-C, No. 6(1981), p. 137-144.
(16) McFarlane, D. and Glover, K., Robust Controller Design Using Normalized Coprime Factor Plant Descriptions, Lecture Notes in Control and Information Sciences, Vol. 138 (1990), Springer-Verlag.
(17) Matsumura, F., Fujita, M. and Okawa, K., Modeling and Control of Magnetic Bearing Systems Achieving a Rotation around the Axis of Inertia, Proc. of 2nd International Symposium on Magnetic Bearings, Tokyo, July, 1990.
(18) Matsumura, F., Fujita, M. and Hatake, K., Output Regulation in Magnetic Bearing Systems by a Dynamic Output Feedback Controller, Trans. IEE of Japan, (in Japanese), Vol. 112-C, No. 10(1992), p. 977-983.